



# Numerical Analysis of Bearing Capacity of Strip Footing Built on Geogrid-Reinforced Sand Slope Over Soft Clay Layer (revised version 3)

Ahmed Hamidi<sup>1</sup> · Khelifa Abbeche<sup>1</sup>

Received: 13 January 2020 / Accepted: 14 May 2020 / Published online: 13 June 2020  
© King Fahd University of Petroleum & Minerals 2020

## Abstract

The paper presents the numerical investigations into the ultimate bearing capacity of the rigid strip footing built on geogrid-reinforced sand over soft clay slope, by means of a detailed parametric study based on a finite element modeling. The parameters investigated are the effect of the vertical distance ratio between consecutive layers ( $h/B$ ), depth ratio of the topmost layer of geogrid ( $u/B$ ), number of geogrid layers ( $N$ ) and the effective depth ratio of reinforcement ( $H/B$ ), where  $B$  is the footing width, and also the effect of friction angle ( $\varphi$ ), density of the sand (loose, moderately dense and dense) and the angle of the slope inclination ( $\beta$ ). A series of finite element analyses were performed on strip footing using the two-dimensional plane strain model using the computer code Plaxis 2D. The soil was represented by nonlinear Mohr–Coulomb model and Cam clay, which is an elastoplastic hyperbolic stress–strain model, while reinforcement was represented by elastic elements. The results illustrated that by increasing the number of reinforcement sheets and the friction angle, the bearing capacity increased, and by decreasing the slope angle, the depth of reinforcement decreased. The improvement in the bearing capacity of the strip footing on a reinforced slope was found to be strongly dependent on the slope angle and the friction angle of the sand. The best improvement in the bearing capacity was noticed if the spacing between the reinforcement layers ( $u/B$ ) and ( $h/B$ ) is small. Numerical results obtained from a series of finite element model tests have been presented and discussed in the paper.

**Keywords** Bearing capacity · Geogrids · Sand · Slope · Soft clay and Strip footing

## List of symbols

BCR	Bearing capacity improvement factor
$i_\beta$	Coefficient of reduction in bearing capacity
$q_{ur}$	Ultimate bearing capacity of reinforced soil
$q_u$	Ultimate bearing capacity of unreinforced soil
$N$	Number of reinforcement layers
$H$	Total depth of reinforcement
$L$	Length of reinforcement
$B$	Foundation width
$u$	Top layer spacing, i.e., spacing between top layer of reinforcement and bottom of footing
$h$	Vertical spacing between reinforcement layers

$N_C$	Factor of cohesion
$I_f$	Friction angle factor

## 1 Introduction

Stabilizing a soil, in the broad sense of term, consists of the soil property modification to improve its technical performance. In the last several years, the soil reinforcement below superficial foundations has been applied to improve the bearing capacity and the settlement of the foundations; in this aspect, several research works were done such as Omar et al [1]; Dash et al [2]; Boushehrian and Hataf [3]; Ghosh and Bera [4, 5]; Patra et al [6, 7]; Sommers and Viswanadham [8]; Madhavi and Somwanshi [9]; Lavas and Ghazavi [10]; Abu-farsakh and Qiming [11, 14]; Boussadia et al [12]; Demir et al [13]; Enas et al [15]; Sahu et al [16]; Kumar et al [17]; Benmebarek et al [18]; Abu-farsakh et al. [11]; Chakraborty and Kumar [19]; Abu-farsakh and Chen [12]; Boussadia et al. [13]; Sadoglu [20]; Nabil and Elshesheny [21]; and Sridhar and Prathap Kumar [22]. Thus, the

✉ Ahmed Hamidi  
ah\_hamidi@outlook.fr  
Khelifa Abbeche  
k.abbeche@univ-batna2.dz

<sup>1</sup> Department of Civil Engineering, Faculty of Technology, University of Batna 2, Batna, Algeria



stabilization of the slopes of soil has become the most interesting field in soil mechanics. As a part of research, various techniques have been suggested to improve slope stability and improve bearing capacity including the geometry of the sloping surface changing, chemical treatment and the use of reinforced soil or the installation of retaining structures such as walls or piles; in this aspect, several research works were done such as Baaziz and Mellas [23] and Emeka et al [24]. The success achieved in reinforcing the weak casings of pavements by geogrid as in soft clay has been described by several authors like Tsukada et al. [25]; Alawaji [26]; Maharaj [27] and Karim et al [28]. The research study established by Tsukada et al [25] was devoted for strengthening the foundations of roads by geogrids. The distributions of pressures as well as the settlement related to the thickness and configuration of the reinforced soil layers were reported by these authors. Moreover, Alawaji [26] studied the effect of reinforcing a block of sand below a collapsible soil where it has been reported that the rate of slump reduction reached a threshold of 75% (after reinforcements). However, Maharaj [27] studied the behavior of strip footings constructed on a reinforced layer of clay where he recognized that compaction was reduced with the increase in the reinforcement size, stiffness and the number of reinforcement layers. Karim et al. [28] performed an experimental study on the influence of using several improving techniques such as fly ash and geogrid on the behavior of soft clayey soil subjected to cyclic loading where it has been reported that the settlement behavior of footing resting on treated models with fly ash and two geogrid layers is better than other improving techniques. Furthermore, several research works such as Huang et al [29]; Yoo [30]; El sawwaf and Nazir [31, 32]; Saeed and Hataf [33]; Sommers and Viswanadham [34]; Choudhary et al [8]; Turker et al [35]; Dhiraj et al [36]; Moradi et al [37]; Abdi et al [38]; and Gholam et al [37] have been carried out to study the behavior of superficial foundations built on sloping sands. However, behavior of a superficial foundations rests on a soil reinforced by rubbing geogrids and located above a soft clay slope. In this aspect, El sawwaf [39] studied the reinforcing effect on the behavior of a strip foundation built on reinforced sand crowd located above a layer of soft clay sloping. It has been reported that the effect of the reinforcing elements on the behavior of the strip footing depends on its location with respect to the crest of the slope, and the reinforcing elements are more effective when the foundation is placed on the crest of the slope.

The objective of this study is to address the aspect of both the bearing capacity improvement and settlement reduction through using both soil replacement and optimum soil reinforcement. The aim is to study the relationships between the footing response and the variable parameters including the depth of the reinforced sand, the location and the number of geogrid layers, vertical spacing of geogrid layers, the depth

of the topmost layer of geogrid. Also, the effects of the angle of the slope inclination and the friction angle of the sand on the footing response were evaluated.

## 2 Finite Element Analyses

A series of two-dimensional finite element analyses (FEA) of the surface strip footing located on geogrid-reinforced sand over soft clay slope under the vertical load were carried out using the geotechnical finite element program Plaxis software package (2D). Plaxis is a set of finite elements intended for the two-dimensional analysis of geotechnical works and rock mechanics. They are used to analyze the problem of excavations, retaining walls, embankments, shallow foundations, tunnels, piles, pile groups, mining and reservoir geomechanics. The software allows for a fully automatic generation of finite element meshes which takes into account the soil layer as well as all structural elements and boundary conditions. In this study, ten series of tests were performed to study the effect of friction angle, the angle of the slope inclination and the inclusion effect of the geogrid layers on the bearing capacity of strip footing. Tests were conducted to find out the best location and the number of the geogrid layers that give the maximum improvement in bearing capacity. Each series was used to study the effect of one parameter, while the other variables were kept constant. The varied conditions include the number of geogrid layers ( $N$ ), vertical spacing between layers ( $h$ ), top layer spacing ( $u$ ), friction angle ( $\varphi$ ) and the angle of the slope inclination ( $\beta$ ). Table 1 and Fig. 1 summarize all the tests programs with varied parameters used. The two-dimensional modeling is performed considering a transversal section of the footing. The initial state of the stresses in the mass is assumed to be geostatic of the  $K_0$  type. The calculation is carried out in several stages: The first is related to the construction of the model, and the second represents the stages of the foundation loading.

### 2.1 Test material

The clay material is supposed to follow a soft soil behavior law and the rupture criterion is considered as the one of Cam clay. The Cam clay model requires a total of five parameters, which are listed as Poisson's ratio ( $\nu$ ), cohesion ( $c$ ), friction angle ( $\varphi$ ), Slope of loading ( $k^*$ ) and Virgin consolidation slope ( $\lambda^*$ ). However, for the sand, the behavior is supposed to be perfect and elastoplastic, where Mohr–Coulomb rupture criterion is used. The Mohr–Coulomb model requires a total of five parameters, which are listed as Poisson's ratio ( $\nu$ ), cohesion ( $c$ ), friction angle ( $\varphi$ ), Young's module ( $E$ ) and dilatancy angle ( $\psi$ ). The Poisson's ratio of the sand was accepted as 0.20, based on the recommendation for

**Table 1** Model test program

Test	Constant parameters			Variable parameters				
	L/B	H/B	d/B	N	h/B	u/B	$\beta$ (°)	$\varphi$ (°)
A01			1	0			15, 20, 25, 30,35	
A02				1			15, 20, 25, 30,35	
A03				2			15, 20, 25, 30,35	
A04				3	0.25		15, 20, 25, 30,35	
A05				4			15, 20, 25, 30,35	
A06				5			15, 20, 25, 30,35	
B01				0			15, 20, 25, 30,35	
B02				1			15, 20, 25, 30,35	
B03				2			15, 20, 25, 30,35	
B04				3	0.50		15, 20, 25, 30,35	
B05				4		0.25	15, 20, 25, 30,35	
B06				5			15, 20, 25, 30,35	
C01				0			15, 20, 25, 30,35	
C02				1			15, 20, 25, 30,35	
C03				2			15, 20, 25, 30,35	
C04				3	0.75		15, 20, 25, 30,35	
C05				4			15, 20, 25, 30,35	
C06				5			15, 20, 25, 30,35	
D01				0			15, 20, 25, 30,35	
D02				1			15, 20, 25, 30,35	35
D03				2		0.25	15, 20, 25, 30,35	
D04				3			15, 20, 25, 30,35	
D05				4			15, 20, 25, 30,35	
D06				5			15, 20, 25, 30,35	
E01				0			15, 20, 25, 30,35	
E02				1			15, 20, 25, 30,35	
E03				2			15, 20, 25, 30,35	
E04				3		0.50	15, 20, 25, 30,35	
E05	8	3	1	4	0.25		15, 20, 25, 30,35	
E06				5			15, 20, 25, 30,35	
F01				0			15, 20, 25, 30,35	
F02				1			15, 20, 25, 30,35	
F03				2			15, 20, 25, 30,35	
F04				3		0.75	15, 20, 25, 30,35	
F05				4			15, 20, 25, 30,35	
F06				5			15, 20, 25, 30,35	
G01				0			15, 20, 25, 30,35	
G02				1			15, 20, 25, 30,35	
G03				2			15, 20, 25, 30,35	
G04				3		1	15, 20, 25, 30,35	
G05				4			15, 20, 25, 30,35	
G06				5			15, 20, 25, 30,35	
H01				0			15, 20, 25, 30,35	
H02				1			15, 20, 25, 30,35	
H03				2			15, 20, 25, 30,35	
H04				3			15, 20, 25, 30,35	30
H05				4			15, 20, 25, 30,35	
H06				5			15, 20, 25, 30,35	
I01				0			15, 20, 25, 30,35	

**Table 1** (continued)

Test	Constant parameters			Variable parameters				
	L/B	H/B	d/B	N	h/B	u/B	$\beta$ (°)	$\varphi$ (°)
I02				1	0.25	0.25	15, 20, 25, 30,35	35
I03				2			15, 20, 25, 30,35	
I04				3			15, 20, 25, 30,35	
I05				4			15, 20, 25, 30,35	
I06				5			15, 20, 25, 30,35	
J01				0			15, 20, 25, 30,35	
J02				1			15, 20, 25, 30,35	40
J03				2			15, 20, 25, 30,35	
J04				3			15, 20, 25, 30,35	
J05				4			15, 20, 25, 30,35	
J06				5			15, 20, 25, 30,35	

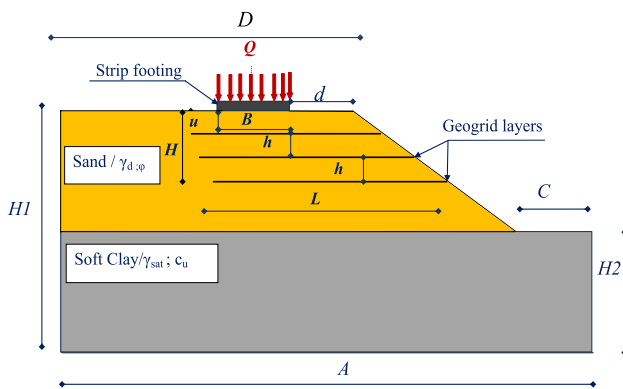


**Fig. 1** Geometric parameters of reinforced sand slope overlying soft clay

medium density sand from Kumar and Madhusudhan [40]. The material parameters adopted in the analysis are presented in Table 2. The foundation is supposed to follow a linear elasticity law where the Young’s modulus is equal to 32,000 MPa; Poisson’s ratio of 0.2 and the density is equal to 25 kN/m<sup>3</sup>. Geogrid reinforcement, which is generally

used to increase bearing capacity, has only tensile stiffness (EA). The geogrid reinforcement was simulated with a five-node bar element by using the geogrid option of Plaxis 2D. The interface between soil and geogrid was defined as fully bonded interface (reduction factor,  $R_i = 1$ ). The physical and mechanical properties of geogrid are given in Table 3.

**2.2 Meshes**

In all cases, the first elaborated meshes were considered relatively coarse and were based on fifteen noded triangular elements with a twelve point Gaussian integration rule to calculate the element stiffness matrices. A refined mesh was adopted to guarantee a better representation of the stress field around the foundation and geogrid layers. For all the models, the boundary conditions in displacements are similar: null vertical displacements at the base of the mass (at 10 B of depth) and null horizontal displacements on the vertical borders of the model. Table 4 and Fig. 2 present the geometric characteristics of FE models in each studied case. All these meshes are built according to the same principle of configuration.

**Table 2** Physico-mechanical properties of the studied soil

Parameters	Name	Sand 1	Sand 2	Sand 3	Soft clay	Unit
Model type		Mohr–Coulomb	Mohr–Coulomb	Mohr–Coulomb	Cam clay	
Dry density	$\gamma$	16	17	19	17	[kN/m <sup>3</sup> ]
Wet density	$\gamma_{sat}$	19	19	21	18	[kN/m <sup>3</sup> ]
Poisson coefficient	$\nu$	0.3	0.30	0.3	0.30	–
Cohesion	$c$	1	1	1	50	[kN/m <sup>2</sup> ]
Angle of friction	$\varphi$	30°	35°	40°	1	[°]
Angle of dilatation	$\psi$	0°	5°	10°	0	[°]
Young’s module	$E$	$2.73 \times 10^4$	$3.65 \times 10^4$	$4.56 \times 10^4$	–	[kN/m <sup>2</sup> ]
Slope of loading	$K^*$	–	–	–	0.15	[–]
Virgin consolidation slope	$\lambda^*$	–	–	–	0.01	[–]

**Table 3** Physico-mechanical properties of the geogrid

Material type	Polyester/ PET trans- parent
Weight per area [g/m <sup>2</sup> ]	380
Tensile strength [kN/m]	20 ≤ R <sub>T</sub> ≤ 80
Lengthening [%]	20 ≤ Δ <sub>L</sub> ≤ 80
Tensile strength at 1% elongation [kN/m]	16
Tensile strength at 2% elongation [kN/m]	28
Tensile strength at 5% elongation [kN/m]	56
Opening of the stitches [mm × mm]	73 × 30
Lengthening before service [%]	0
Roll dimension width and length [m × m]	4.75 × 100
EA [KPa]	500

### 2.3 Calculation Stages and Loading Increment

The simulation of the problem was carried out in three stages: The first corresponds to the creation of the initial state, the second is the construction of the sand layers with the laying of the reinforcement elements, and the last is the loading of the strip footing. The initial state corresponds to a state of stress such that the vertical stress balances the land weight and the effective horizontal stress is a fraction of the effective vertical stress. The resting earth pressure in this case (sloping ground) was calculated from the gravitational force according to the Plaxis code. For each simulation model, the solicitation is carried out in a controlled displacement in the form of an increment of uniform displacements, up to a maximum value equal to (B/10), applied on the lower part of the footing, which corresponds conventionally to settlement of the foundation, when exceeding the bearing capacity of the soil.

### 3 Validation of the Model in Finite Elements

During the finite element model definition process, multi-tude approximations are applied (mesh, finite element type, number of nodes, behavior laws, etc.).

**Table 4** Characteristics of meshes in the different studied FE models

Slope β(°)	Number of element	Number of nodes	Finite element size [m]	Dimension of the model in FE [m]				
				H1	H2	A	D	C
15	2519	20,499	336.480 × 10 <sup>-3</sup>	10	5	28.52	10	0.00
20	2657	21,599	306.740 × 10 <sup>-3</sup>	10	5	25	11	0.00
25	2373	19,279	304.480 × 10 <sup>-3</sup>	10	5	22	10	2.00
30	2401	19,503	302.700 × 10 <sup>-3</sup>	10	5	22	12	1.63
35	2483	20,183	297.66 × 10 <sup>-3</sup>	10	5	22	12	3.00

To validate our numerical model, we compared the capacity factor values due to cohesion (N<sub>c</sub>) of a flexible strip footing obtained by finite element method to the ones given by the literature or the classical theory of the bearing capacity. The simulation of a flexible strip footing resting on a purely coherent and undrained soil layer (φ<sub>u</sub> = 0 and ν = 0.5) is a very simple example of validation. In this validation, the sand layer is replaced by a purely coherent and undrained clay layer having the same parameters as the lower soil layer, where the ratio c<sub>1</sub>/c<sub>2</sub> = 1. Then, we impose a uniform vertical pressure on a strip footing realized on the ground surface, and it is placed on the left vertical part of the model, which means that the effect of the slope is much neglected, and the footing behaves as a foundation built on a horizontal floor. The maximum pressures that have been applied are 140 kPa for soft clay, 350 kPa for firm clay and 1300 kPa for stiff clay.

The different mechanical characteristics that have been taken into consideration according to Mohr–Coulomb criteria are: c<sub>u</sub> = 20 kPa and E<sub>u</sub> = 5 MPa for soft clay, c<sub>u</sub> = 50 kPa and E<sub>u</sub> = 20 MPa for firm clay, and on the other side c<sub>u</sub> = 200 kPa and E<sub>u</sub> = 40MP for steep clay. The general formula of the bearing capacity of a flexible footing for a purely coherent soil (φ<sub>u</sub> = 0) is written as.

$$q_1 = N_c \times C_u; \quad N_\gamma = N_q = 0, \tag{1}$$

and the factor of cohesion is given by:

$$N_c = q_{lc}/C_u. \tag{2}$$

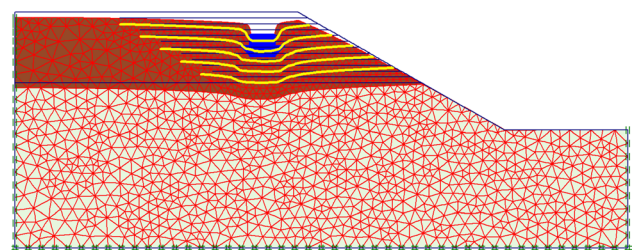


**Fig. 2** Numerical model test with generated mesh and boundary conditions

Table 5 presents the test results corresponding to the cohesion factor of the bearing capacity of the different finite element models, compared to the ones given by Prandtl [41], Merifield et al. [42, 43] and Michalowski [44]. According to the calculation results in a flexible strip foundation, it was noticed that the factor due to cohesion and given by FEM (Plaxis) is almost the same as the one given by the literature and classical theory at a maximum deviation of 3%. This very good concordance can be considered as a validation of the finite element model designed by this study.

### 4 Results and Discussions

Over the last 30 years, several research projects have been carried out to study the behavior of geosynthetically reinforced foundation soils. All of these works indicated that the use of geogrids increases the bearing capacity and decreases settlement of foundations. A total of 60 numerical tests were carried out on strip footing built on geogrid-reinforced sand slope over soft clay layer. The effect of inclusion of geogrid reinforcement on bearing capacity of the strip footing was presented using non-dimensional factor, called bearing capacity ratio due to reinforcement (BCR). This factor is defined as the ratio of the footing ultimate pressure with the slope reinforced ( $q_{u \text{ reinforced}}$ ) to the footing ultimate pressure in tests without slope reinforcement ( $q_{u \text{ unreinforced}}$ ) (Eq. 3)

$$BCR = q_{ur} / q_u, \tag{3}$$

where  $q_{ur}$  is the bearing capacity of soil after reinforcement and  $q_u$  is the bearing capacity of the soil before reinforcement.

#### 4.1 Effect of Reinforcement Depth

The reinforcement depth is a very important parameter in terms of improving the bearing capacity of the reinforced surface foundations. In this aspect, we examined numerous series of tests on sand reinforced by many layers of geogrid.

In these tests, the vertical spacing between the bottoms of the footing and the first reinforcing element ( $u$ ) was set at 0.25 B, and the vertical spacing between consecutive reinforcing elements ( $h$ ) was set at 0.25 B. Then, the value of the slope angle ( $\beta$ ) was varied as follows: 15°, 20°, 25°, 30° and 35°, and the depth of the reinforced zone has been varied between 0.25 and 3 B. The sand that has been simulated is moderately dense sand (sand 2 Table 2).

Figure 3 presents the variation of the improvement factor (BCR) with the vertical spacing between the reinforcing elements. It can be recognized that the increase in the depth of the reinforcement zone ( $H$ ) results from a considerable increase in the factor (BCR), regardless of the slope ( $\beta$ ). However, we noticed that the depth of the reinforcement zone has no effect on the variation of the improvement factor (BCR) when it exceeds the threshold distance, noted  $H_{lim}$ .

Figure 4 presents the variation of the vertical pressure calculated with the variation of the vertical displacement ( $s/B$ ). It has been found that the increase in the numbers of reinforcing elements results from a considerable increase in the vertical pressure whatever the slope ( $\beta$ ). The values of the reinforcement depth ( $H_{lim}$ ) related to this test are: 1.25 B, 1.50 B, 2.0 B, 2.25 B and 2.75 B, according to the

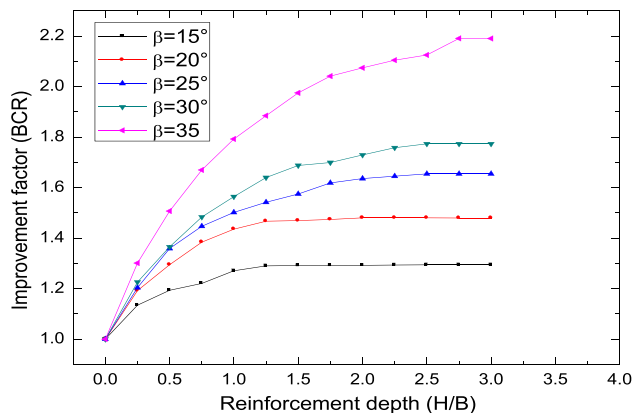
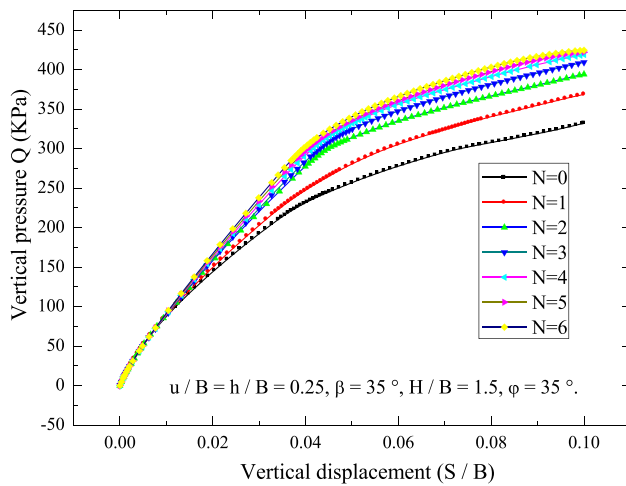


Fig. 3 Improvement factor (BCR) variation in terms of reinforcement depth (H/B).  $u/B = h/B = 0.25, \varphi = 35^\circ$

Table 5 Cohesion factor calculation results of the bearing capacity of a strip footing subjected to a uniform vertical pressure

Slope $\beta$ [°]	Present study			Solution exacted prenatal	Lower bound Merifield et al. [42]	Upper bound Merifield et al [42]	FEM Merifield et al. [43]	Michalowski [44]
	Case (1)	Case (2)	Case (3)					
15	5.28	5.27	5.28	5.14	4.94	5.32	5.11	5.141
20	5.30	5.29	5.29					
25	5.23	5.28	5.28					
30	5.31	5.31	5.30					
35	5.13	5.24	5.24					





**Fig. 4** Load curve of vertical pressure in relation to displacement (S/B)

different slopes that have been studied, 15°, 20°, 25°, 30° and 35°, respectively. The maximum values of the departure improvement factor (BCR) that have been found at are: 1.29, 1.48, 1.64, 1.78, 2.2, corresponding to the different slopes ( $\beta$ ): 15°, 20°, 25°, 30° and 35°, respectively.

### 4.2 Effect of Geogrid Layer Number

To understand the effect of the number of reinforcing elements, we examine a series of tests on sand reinforced by several sheets of geogrid. In this test, we set the vertical spacing between the bottoms of the footing and the first reinforcing element ( $u$ ) at 0.25 B and the vertical spacing between consecutive reinforcing elements ( $h$ ) at 0.25 B. Then, we varied the value of the angle of the slope ( $\beta$ ) as follows: 15°, 20°, 25°, 30° and 35°, and the depth of the reinforced zone was varied between 0.25 and 3 B. The sand that has been simulated is moderately dense sand (sand 2 Table 2).

Figure 5 presents the variation of the improvement factor (BCR) with the number of reinforcement elements ( $N$ ). It can be noticed that the increase in the improvement factor (BCR) results from a considerable increase in reinforcement elements, regardless of the slope ( $\beta$ ). Thus, we have found the existence of a threshold number of reinforcement elements, noted  $N_{lim}$ , beyond which the number of reinforcement has no effect on the variation of the improvement factor (BCR). This is consistent with previous research work of strip or square footing over dry sand which demonstrated that there are a threshold number of geogrid layers after which the bearing capacity ratio (BCR) remains constant (Omar et al. [1]; Das et al. [2]; El Sawwaf [39]). The threshold values of the number of reinforcing elements  $N_{lim}$ , which have been identified are: 4, 5, 7, 9, 11 according to the different studied

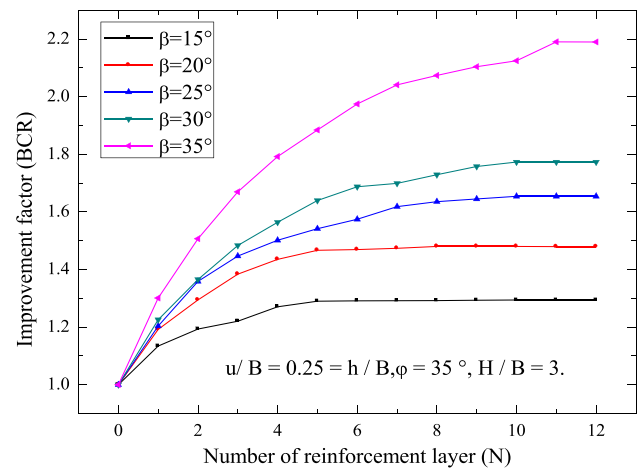


**Fig. 5** Improvement factor (BCR) variation in relation to geogrid layer number (N)

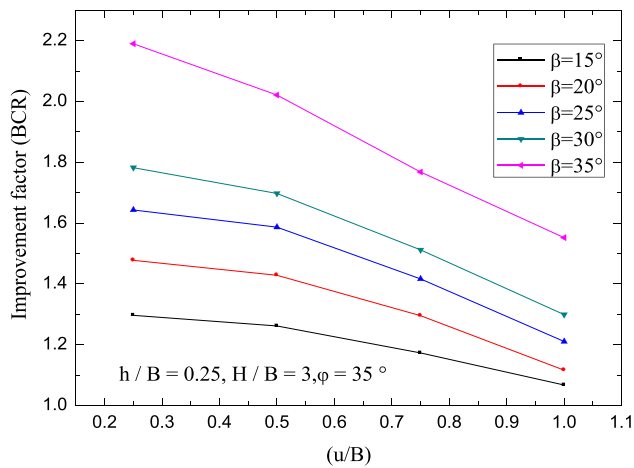
slopes: 15°, 20°, 25°, 30° and 35°, respectively. The maximum values of the improvement factor (BCR) are 1.29, 1.48, 1.64, 1.78 and 2.20 corresponding to the different slopes of the studied model, 15°, 20°, 25°, 30° and 35°, respectively.

### 4.3 Effect of Vertical Spacing of the Geogrid

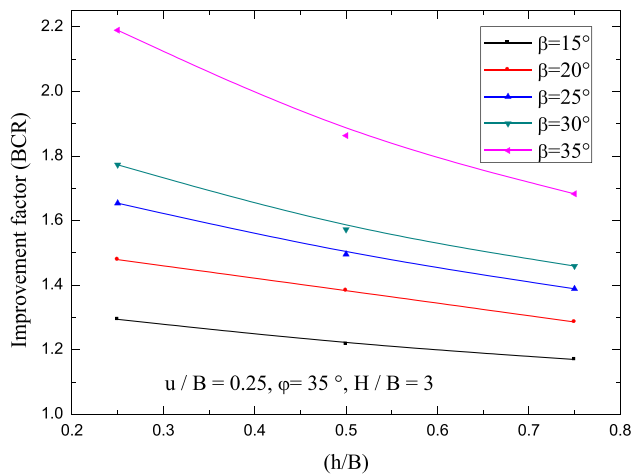
To evaluate the effect of the spacing between the reinforcing elements, we examined two series of tests. In the first series of tests, we set the ratio ( $h/B$ ) at 0.25 and the depth of the reinforcement zone ( $H$ ) at 3 B. However, the vertical spacing between the bottoms of the footing and the first reinforcing element ( $u/B$ ) was varied by the following values: 0.25, 0.50, 0.75 and 1.00, and the slope ( $\beta$ ) by: 15°, 20°, 25°, 30° and 35°. In the second series of tests, we set the ratio ( $u/B$ ) at 0.25 and the reinforcement depth ( $H$ ) at 3B, and we varied the vertical spacing between consecutive reinforcing elements ( $h/B$ ) as follows: 0.25, 0.50 and 0.75, and the slope ( $\beta$ ) by the following values: 15°, 20°, 25°, 30° and 35°. The sand that has been simulated is moderately dense sand with a 35° angle of friction (sand 2) as shown in Table 2.

Figure 6 presents the variation of improvement factor (BCR) with the vertical spacing ( $u/B$ ) of each slope ( $\beta$ ) of the studied model. It has been observed that the increase in the spacing between the bottoms of the footing and the first reinforcing element induces a decrease in the improvement factor (BCR) value, whatever the slope ( $\beta$ ). It decreased from 2.20 to 1.54 when the slope ( $\beta$ ) is equal to 35°, from 1.78 to 1.29 when the slope ( $\beta$ ) is equal to 30°, from 1.64 to 1.21 when ( $\beta$ ) is equal to 25°, and from 1.30 to 1.06 when the slope ( $\beta$ ) is equal to 15°.

Figure 7 presents the variation of the improvement factor (BCR) with the vertical spacing between the reinforcing elements ( $h/B$ ), of each slope ( $\beta$ ) of the studied model. A



**Fig. 6** Improvement factor variations in terms of vertical spacing ( $u/B$ )



**Fig. 7** Improvement factor (BCR) variation in terms of vertical spacing ( $h/B$ )

considerable decrease in the improvement factor (BCR) has been observed when the spacing between the reinforcing elements increases, whatever the slope ( $\beta$ ). The values of the latter decreased from 2.20 to 1.68 when the slope ( $\beta$ ) is equal to  $35^\circ$ , from 1.78 to 1.45 when the slope ( $\beta$ ) is equal to  $30^\circ$ , from 1.65 to 1.38 when ( $\beta$ ) is equal to  $25^\circ$ , and from 1.28 to 1.16 when the slope ( $\beta$ ) is equal to  $15^\circ$ . These results are similar to the results obtained by Shin & Das [45] and Qiming Chen [46].

#### 4.4 Effect of Slope $\beta$

The particular configuration of a foundation located near a slope is a frequently encountered case in practice. This problem has been the subject of full-scale tests or centrifuged or normal gravity models. To evaluate the effect of the slope

( $\beta$ ) on the variation of the bearing capacity of reinforced soils, we examined a series of tests of moderately dense sand reinforced by several layers of geogrid, with an angle of friction ( $\varphi$ ) equal to  $35^\circ$ . The principle of this test is to set the vertical spacing between the bottoms of the footing and the first reinforcing element ( $u$ ) at  $0.25 B$ , the vertical spacing between the consecutive reinforcement elements ( $h$ ) at  $0.25 B$  and the depth of the reinforced zone at  $3 B$ . Then, we varied the angle of the slope ( $\beta$ ) by the following values:  $15^\circ$ ,  $20^\circ$ ,  $25^\circ$ ,  $30^\circ$  and  $35^\circ$ . The evaluation of the effect of the slope ( $\beta$ ) on the variation of the bearing capacity has been expressed by a non-dimensional term called the coefficient of reduction in bearing capacity ( $i_\beta$ ). The value of the latter is estimated by the ratio between the bearing capacities of a top slope, with the bearing capacity of a small slope ( $\beta$ ), as expressed in Eq. (4)

$$i_\beta = q_{\beta_{\max}} / q_{\beta_{\min}} \quad (4)$$

In this part of work, we supposed that the slope is weak when ( $\beta$ ) is equal to  $15^\circ$  and steep when ( $\beta$ ) is equal to  $20^\circ$ ,  $25^\circ$ ,  $30^\circ$  and  $35^\circ$ .

Figure 8 presents the variation of the reducing coefficient of the bearing capacity ( $i_\beta$ ) as a function of the slope ( $\beta$ ) of a foundation in the vicinity of the slope. For this purpose, it has been found that the reducing coefficient of the bearing capacity decreases when the angle of inclination of the slope ( $\beta$ ) increases, whatever the variation in the number of reinforcement layers. The results of the present investigation shows that a large influence of slope ( $\beta$ ) on the bearing capacity and the groundbreaking mechanism. The values obtained from the reducing coefficient of the bearing capacity ( $i_\beta$ ) are varied between 0.96 and 0.84 for a slight slope at  $20^\circ$ , and between 0.82 and 0.55 for a steep slope at  $35^\circ$ .

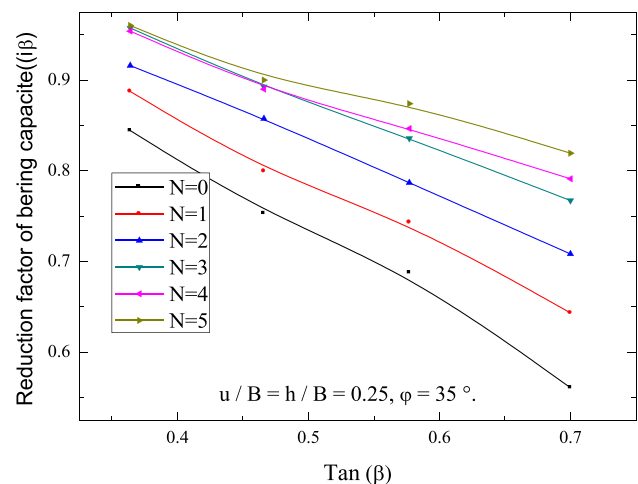


**Fig. 8** Variation of reduction coefficient of bearing capacity ( $i_\beta$ ) in relation to the Slope ( $\beta$ )



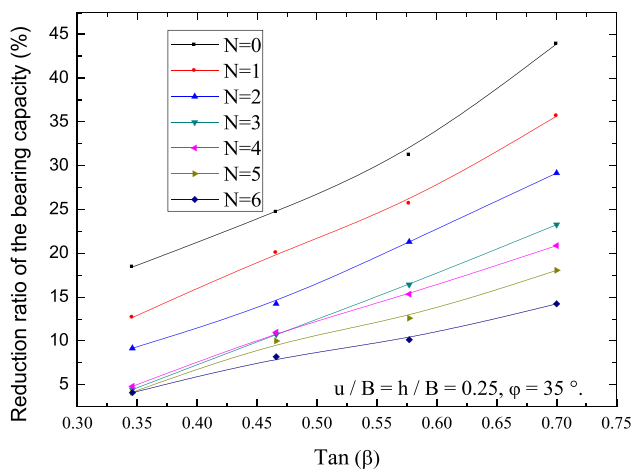


Fig. 9 Rate of reduction in bearing capacity related to the slope (β)

Moreover, it was found that beyond the reinforcement layer  $N=3$ , the reducing coefficient of bearing capacity becomes very low, whatever the slope.

Figure 9 presents the variation of the rate of the bearing capacity reduction with the slope (β). A considerable increase in this rate is noticed when the sand is unreinforced, and a weak increase is observed for a reinforced sand, which can be explained by the important number of reinforcing elements. The maximum rate found is of the order of 44% for unreinforced sand and 14.5% for reinforced sand related to an important number of reinforcing elements.

### 4.5 Effect of Friction Angle (φ)

During the construction of sand layers reinforced by geosynthetics (geogrid), the physical and mechanical parameters of the soil are very important factors with regard to the dimensioning of shallow foundations. In the present work, we treated the angle of friction of the sand factor which represents one of the most affecting parameters. For this purpose, we examined a series of tests that use three different types of sand (loose, dense and moderately dense) reinforced by several sheets of geogrid. The principle of this test is to fix the vertical spacing between the bottoms of the footing and the first reinforcing element ( $u$ ) at 0.25  $B$ , the vertical spacing between the consecutive reinforcing elements ( $h$ ) at 0.25  $B$  and the depth of the reinforced zone ( $H$ ) at 3 $B$ . Then, we varied the angle of the slope (β) by the following values: 15°, 20°, 25°, 30° and 35°, when the angle of friction (φ) assumed the values 30°, 35° and 40°. The evaluation of the effect of the angle of friction on the bearing capacity was expressed by a non-dimensional term called friction angle factor ( $I_f$ ). The value of the latter is estimated by the ratio between the bearing capacities of a high angle of friction with the bearing capacity of a low

angle of friction, as indicated in Eq. (5), where  $q_{φmax}$  is the bearing capacity of soils with a high friction angle of 35° and 40°, and  $q_{φmin}$  is the bearing capacity of soils with a low angle of friction of 30°.

$$i_f = q_{φmax} / q_{φmin} \tag{5}$$

Figure 10 presents the variation of the improvement factor (BCR) with the internal friction angle of the sand. A considerable increase in the factor of improvement in the bearing capacity has been observed when the angle of friction (φ) increases in all cases. It is interesting to note that the results obtained by the present study indicate a considerable effect of the soil internal friction angle (φ) on the improvements factor (BCR).

The results of this study shows that with the increase in the internal friction angle (φ) of the soil, the coefficient of the angle of friction ( $I_f$ ) increases as shown in Fig. 11, whatever the slope (β). The values of the latter are varied linearly from 1 to 1.76 in all the studied cases, with a maximum variation of 0.07 in the case where the angle of friction is equal to 40°.

Figure 12 presents the effect of the angle of friction on the variation of the rate of the bearing capacity improvements. In this part of work, we notice there is a great improvement in the bearing capacity related to the increase in the friction angle of the sand, whatever the number of reinforcing elements. The rate of improvement varied between 300 and 65% in the case of dense sand having with an angle of friction of 40°.

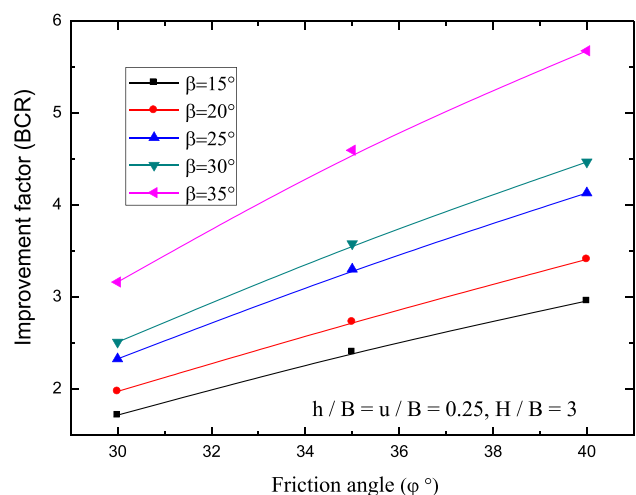
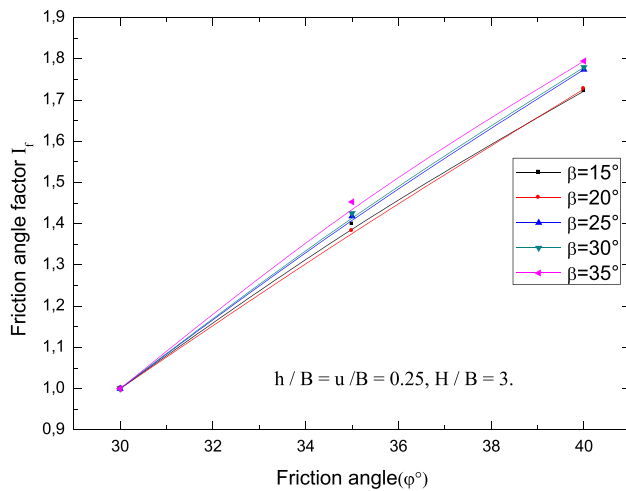
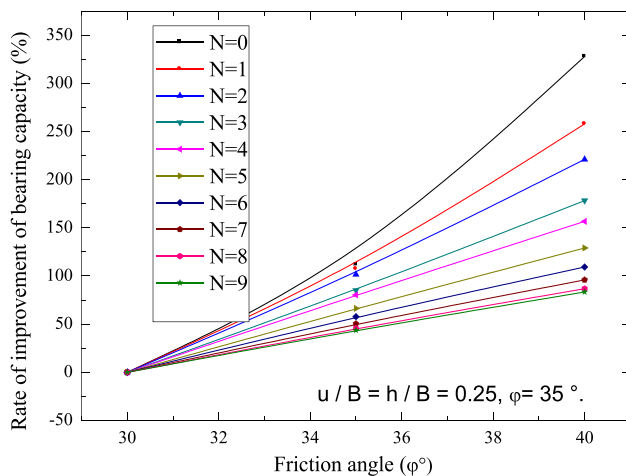


Fig. 10 Variation of improvement factor (BCR) in terms of friction angle φ



**Fig. 11** Variation of friction angle factor in terms of internal friction angle ( $\phi$ )



**Fig. 12** Rate of improvement in the bearing capacity in terms of friction angle ( $\phi$ )

## 5 Conclusions

The numerical investigations were carried out to find the ultimate bearing capacity of a strip footing resting on replaced sand layer (partially replaced) constructed on a soft clay slope, by means of a detailed parametric study based on a finite element modeling. The main results obtained from this numerical investigation are summarized as follows.

1. Soil improvement in soft clay ground slope by partial replacement with sand layer significantly increases the load bearing capacity of a footing placed near the crest of sloping ground.

2. The optimum depths of reinforcement ( $H_{lim}$ ) that were found corresponding to the following slopes:  $15^\circ$ ,  $20^\circ$ ,  $25^\circ$ ,  $30^\circ$  and  $35^\circ$  of the studied models, are, respectively:  $1.25 B$ ,  $1.50 B$ ,  $2.0 B$ ,  $2.25 B$  and  $2.75 B$ .
3. The optimum values of the number of reinforcement elements ( $N_{lim}$ ) that have been observed are: 4, 5, 7, 9 and 11 related to the following slopes:  $15^\circ$ ,  $20^\circ$ ,  $25^\circ$ ,  $30^\circ$  and  $35^\circ$  of each studied model, respectively.
4. Reducing the distance between the first reinforcement layer and the underside of the footing increases the bearing capacity of the reinforced soil. Effective depth ( $u$ ) of the first reinforcing layers measured from the bottom of the footing is  $0.25 B$ .
5. Reducing the distance between the reinforcing layers ( $h$ ) increases the bearing capacity of the reinforced soil. Within the effective reinforced zone, the optimum spacing between the reinforcing layers is  $0.25 B$ .
6. The use of reinforcement layers reduces the effect of the slope ( $\beta$ ) on the bearing capacity; this reduction is varied between 15% and 45%, which is related to the following slopes:  $15^\circ$  and  $35^\circ$ , respectively.
7. The increase in the friction angle of the sand increases the bearing capacity of the reinforced and unreinforced soil, whatever the slope ( $\beta$ ).

## References

1. Omar, M.; Das, B.; Puri, V.; Yen, S.: Ultimate bearing capacity of shallow foundations on sand with geogrid reinforcement. *Can. Geotechn. J.* **30**(3), 545–549 (1993). <https://doi.org/10.1139/t93-046>
2. Dash, S.; Sireesh, S.; Sitharam, T.: Model studies on circular footing supported on geocell reinforced sand underlain by soft clay. *Geotext. Geomembr.* **21**(4), 197–219 (2003). [https://doi.org/10.1016/S0266-1144\(03\)00017-7](https://doi.org/10.1016/S0266-1144(03)00017-7)
3. Boushehrian, J.H.; Hataf, N.: Experimental and numerical investigation of the bearing capacity of model circular and ring footings on reinforced sand. *Geotext. Geomembr.* **21**(4), 241–256 (2003). [https://doi.org/10.1016/S0266-1144\(03\)00029-3](https://doi.org/10.1016/S0266-1144(03)00029-3)
4. Ghosh, A.; Bera, A.K.: Bearing capacity of square footing on pond ash reinforced with jute-geotextile. *Geotext. Geomembr.* **23**(2), 144–173 (2005). <https://doi.org/10.1016/j.geotextmem.2004.07.002>
5. Bera, A.K.; Ghosh, A.: Regression model for bearing capacity of a square footing on reinforced pond ash. *Geotextiles Geomembr.* **23**(2), 261–286 (2005). <https://doi.org/10.1016/j.geotextmem.2004.09.002>
6. Patra, C.R.; Das, B.M.; Atalar, C.: Bearing capacity of embedded strip foundation on geogrid-reinforced sand. *Geotext. Geomembr.* **23**(5), 454–462 (2005). <https://doi.org/10.1016/j.geotextmem.2005.02.001>
7. Patra, C.R.; Das, B.M.; Bhoi, M.; Shin, E.C.: Eccentrically loaded strip foundation on geogrid reinforced sand. *Geotext. Geomembr.* **24**(4), 254–259 (2006). <https://doi.org/10.1016/j.geotextmem.2005.12.001>
8. Sommers, A.N.; Viswanadham, B.V.S.: Centrifuge model tests on the behavior of strip footing on geotextile-reinforced slopes. *Geotext.*



- Geomembr. **27**, 497–505 (2009). <https://doi.org/10.1016/j.geotextmem.2009.05.002>
9. Madhavi, L.; Somwanshi, A.: Bearing capacity of square footings on geosynthetic reinforced sand. *Geotext. Geomembr.* **27**, 281–294 (2009). <https://doi.org/10.1016/j.geotextmem.2009.02.001>
  10. Lavas, A.; Ghazavi, M.: Behavior of closely spaced square and circular footings on reinforced sand. *Soils Found.* **52**(1), 160–167 (2012). <https://doi.org/10.1016/j.sandf.2012.01.006>
  11. Abu-Farsakhan, M.; Qiming, C.; Radhey, S.: An experimental valuation of the behavior of footings on geosynthetic-reinforced sand. *Soils Found.* **53**(2), 335–348 (2013). <https://doi.org/10.1016/j.sandf.2013.01.001>
  12. Qiming, C.; Abu-Farsakh, M.: Ultimate bearing capacity analysis of strip footings on reinforced soil foundation. *Soils Found.* **55**(1), 74–85 (2015). <https://doi.org/10.1016/j.sandf.2014.12.006>
  13. Bouassida, M.; Jellali, B.; Lyamin, A.: Ultimate bearing capacity of a strip footing on ground reinforced by a trench. *Int. J. Geomech.* **15**(3), 06014021 (2014). [https://doi.org/10.1061/\(ASCE\)GM.1943-5622.0000418](https://doi.org/10.1061/(ASCE)GM.1943-5622.0000418)
  14. Demir, A.; Yildiz, A.; Laman, M.; Ornek, M.: Experimental and numerical analyses of circular footing on geogrid-reinforced granular fill underlain by soft clay. *Acta Geotech.* **9**(4), 711–723 (2014). <https://doi.org/10.1007/s11440-013-0207-x>
  15. Enas, B.A.; Mohd, R.T.; Fathi, M.A.: Behavior of strip footing on reinforced sand slope. *J. Civ. Eng. Manag.* **21**(3), 376–383 (2015). <https://doi.org/10.3846/13923730.2014.890646>
  16. Sahu, R.; Patra, C.; Das, B.; Sivakugan, N.: Ultimate bearing capacity of rectangular foundation on geogrid-reinforced sand under eccentric load. *Int. J. Geotech. Eng.* **10**(1), 52–56 (2016). <https://doi.org/10.1179/1939787915Y.0000000008>
  17. Sanjeev, K.; Anil, K.S.; Sanjeev, N.: Performance of circular footing on expansive soil bed reinforced with geocells of Chevron pattern. *Civ. Eng. J.* **5**(11), 2333–2348 (2019)
  18. Benmebarek, S.; Djeridi, S.; Benmebarek, N.: Effect of geosynthetic reinforcement filled with aggregate on the bearing capacity of sand. *Int. J. Geotech. Eng.* **12**(6), 537–545 (2018)
  19. Chakraborty, M.; Kumar, J.: Bearing capacity of circular foundations reinforced with geogrid sheets. *Soils Found.* **54**(4), 820–832 (2014). <https://doi.org/10.1016/j.sandf.2014.06.013>
  20. Sadoglu, E.: Numerical analysis of centrally and eccentrically loaded strip footing on geotextile reinforced sand. *Geosynth. Int.* **22**(3), 225–234 (2015)
  21. Nabil, N.; Elshesheny, A.: Numerical Evaluation of Bearing Capacity of Square Footing on Geosynthetic Reinforced Sand. In: Proceedings of the International Conference on Civil, Structural and Transportation Engineering Ottawa, Ontario, Canada. May 4–5, paper No. 143 (2015).
  22. Sridhar, R.; Prathap Kumar, M.T.: Behavior of model footing resting on sand reinforced with number of layers of coir geotextile. *Innov. Infra Struct. Solut.* **2**, 50–58 (2017)
  23. Baaziz, S.E.; Mellas, M.: Walls influence of parameters the wall on reinforced soil segmental. *Civ. Eng. J.* **2**(6), 395–411 (2017)
  24. Arinze, E.E.; Agunwamba, J.C.; Mama, B.O.: Deformation Behavior of Erodible Soil Stabilized with Cement and Quarry Dust. *Emerg. Sci. J.* **2**(6), 383–387 (2018)
  25. Tsukada, Y.; Isoda, T.; Yamanouchi, T.: Geogrid subgrade reinforcement and deep foundation. Proceedings of the Geosynthetics Case Histories ISSMFE technical Committee. TC9, Yono City, Japan (1993)
  26. Alawaji, H.: Settlement and bearing capacity of geogrid-reinforced sand over collapsible soil. *Geotext. Geomembr.* **19**, 75–88 (2001). [https://doi.org/10.1016/s0266-1144\(01\)00002-4](https://doi.org/10.1016/s0266-1144(01)00002-4)
  27. Maharaj, D.: Nonlinear finite element analysis of strip footing on reinforced clay. *Electron. J. Geotech. Eng.* **8**, (2003).
  28. Karim, H.H.; Samueel, Z.W.; Jassem, A.H.: Behavior of soft clayey soil improved by fly ash and geogrid under cyclic loading. *Civ. Eng. J.* **6**(2), 225–237 (2020)
  29. Huang, C.; Tatsuoka, F.; Sato, Y.: Failure mechanisms of reinforced sand slopes loaded with a footing. *Soils Found.* **24**(2), 27–40 (1994). [https://doi.org/10.3208/sandf1972.34.2\\_27](https://doi.org/10.3208/sandf1972.34.2_27)
  30. Yoo, C.: Laboratory investigation of bearing capacity behavior of strip footing on geogrid-reinforced sand slope. *Geotext. Geomembr.* **19**(5), 279–298 (2001). [https://doi.org/10.1016/S0266-1144\(01\)00009-7](https://doi.org/10.1016/S0266-1144(01)00009-7)
  31. El Sawwaf, M.; Nazir, A.K.: Behavior of repeatedly loaded rectangular footings resting on reinforced sand. *Alex. Eng. J.* **49**(12), 349–356 (2010). <https://doi.org/10.1016/j.aej.2010.07.002>
  32. El Sawwaf, M.; Nazir, A.K.: Cyclic settlement behavior of strip footings resting on reinforced layered sand slope. *J. Adv. Res.* **3**(4), 315–324 (2011). <https://doi.org/10.1016/j.jare.2011.10.002>
  33. Saeed, A.; Hataf, N.: Bearing capacity of strip footings on sand slopes reinforced with geogrid and grid-anchor. *Geotext. Geomembr.* **27**, 217–226 (2009). <https://doi.org/10.1016/j.geotextmem.2008.11.011>
  34. Choudhary, A.K.; Jha, N.J.; Gill, K.S.: Laboratory investigation of bearing capacity behavior of strip footing on reinforced flyash slope. *Geotext. Geomembr.* **28**, 393–402 (2010). <https://doi.org/10.1016/j.geotextmem.2009.09.007>
  35. Turker, E.; Sadoglu, E.; Cure, E.; Uzuner, B.A.: Bearing capacity of eccentrically loaded strip footings close to geotextile-reinforced sand slope. *Can. Geotech. J.* **51**(8), 884–895 (2014). <https://doi.org/10.1139/cgj-2014-0055>
  36. Dhiraj, P.; Sunil, P.; Sanjay, T.: Behavior of strip footing on geogrid reinforced slope subjected to eccentric load. *Inte. J. Innov. Res. Sci. Eng. Technol.* **6**(6), 10929–10936 (2017). <https://doi.org/10.15680/IJRSET.2017.060614>
  37. Moradi, G.H.; Abdolmaleki, A.; Soltani, P.: Small-and large-scale analysis of bearing capacity and load-settlement behavior of rock-soil slopes reinforced with geogrid-box method. *Geomech. Eng.* **18**(3), 315–328 (2019). <https://doi.org/10.12989/gae.2019.18.3.315>
  38. Abdi, A.; Abbeche, K.; Athmania, D.J.; Bouassida, M.: Effective width rule in the analysis of footing on reinforced sand slope. *Stud. Geotech. Mech.* **41**(1), 42–55 (2019). <https://doi.org/10.2478/sgem-2019-0005>
  39. Mustafa, A.; El Sawwaf, : Behavior of strip footing on geogrid-reinforced sand over a soft clay slope. *Geotext. Geomembr.* **25**, 50–60 (2007). <https://doi.org/10.1016/j.geotextmem.2006.06.001>
  40. Kumar, J.; Madhusudhan, B.N.: Effect of relative density and confining pressure on Poisson ratio from bender and extended elements tests. *Geotechnique* **60**(7), 561–567 (2010). <https://doi.org/10.1680/geot.9.T.003>
  41. Prandtl, L.: Über die Härte plastischer Körper. In *Nachrichten von der Gesellschaft der Wissenschaften zu Göttingen, Mathematisch-Physikalische Klasse*, pp 74–85 (1920)
  42. Merifield, R.S.; Sloan, S.W.; Yu, H.S.: Rigorous plasticity solutions for the bearing capacity of two-layered clays. *Géotechnique*. **49**, 471–490 (1999). <https://doi.org/10.1680/geot.1999.49.4.471>
  43. Merifield, R.S.; Sloan, S.W.; Yu, H.S.: Stability of plate anchors in undrained clay. *Géotechnique*. **51**, 141–153 (2001). <https://doi.org/10.1680/geot.2001.51.2.141>
  44. Michalowski, R.L.: Collapse loads over two-layer clay foundation soils. *Soils Found.* **42**(1), 1–7 (2002). <https://doi.org/10.3208/sandf.42.11>
  45. Das, B.M.; Shin, E.C.: Bearing capacity of strip footing on geogrid reinforced sand. In: Proceedings of the 11th Asian Regional Conference on Soil Mechanics and Geotechnical Engineering. Hong, Rotterdam, pp 189–192 (1999)
  46. Chen, Q.: An experimental study on characteristics and behavior of reinforced soil foundation. These; B.S., Nanjing Architecture and Civil Engineering Institute, China (2007).

